Synchronization of coupled assemblies of relaxation oscillatory electrode pairs

Antonis Karantonis,* Yasuyuki Miyakita, and Seiichiro Nakabayashi
Department of Chemistry, Faculty of Science, Saitama University, Saitama City, Saitama 338-8570, Japan
(Received 3 December 2001; published 2 April 2002)

Spatiotemporal patterns emerging through coupling of identical relaxation oscillatory electrode pairs are studied. Each pair, consisting of an iron anode and a copper cathode, oscillates periodically under fixed applied potential difference conditions. It is shown that the system synchronizes rapidly (within few oscillatory cycles) and differences of natural frequencies as well as boundary effects are compensated. The effect of the geometrical configuration on the dynamic modes is investigated for relatively large assemblies of such oscillatory pairs. When oscillators are coupled through neighboring electrodes, the response is synchronized by a simultaneous formation of groups. The formation of groups due to enhancement or inhibition of the oscillations depends on the relative position of interacting anodes and cathodes. The behavior of the system is compared with the response of coupled relaxation cells of neurophysiological interest.

DOI: 10.1103/PhysRevE.65.046213 PACS number(s): 82.40.Bj, 05.45.−a

I. INTRODUCTION

Neurons can be either excitatory or inhibitory depending on the response of their postsynaptic membrane potential. Excitation facilitates the generation of an action potential on the postsynaptic neuron whereas inhibition usually impedes the generation of an action potential. Frequently, excitation and inhibition refers to the average action of a neuron, not the action of an individual synapse [1]. Collective synchronization, asynchronous, partially synchronous response, and oscillatory correlation of coupled neural oscillators are just some types of dynamical behavior with implications in neurobiological sciences [2–5].

Phase models, in which synchrony is through phase pulling, are often used as paradigms for coupled neural oscillators [6,7]. Nevertheless, it was shown that the synchronization mechanism for relaxation neurons can be a lot different than the coupling of oscillators with a more sinusoidal character [8–12]. It was actually proved analytically that for coupled relaxation oscillators and for sufficiently close initial conditions, the properties of the oscillators determine the rate of approach to synchrony, almost independent of the size of coupling [9,10]. The major result of the fast threshold modulation theory by Somers and Kopell, concerning the in-phase synchronized solution of coupled excitatory relaxation oscillators, can be summarized as follows: It is stable, it is persistent in the presence of nonuniformity of natural frequencies, and, it has a rapid rate of convergence.

Synchronization of relaxation neurons is accompanied by several features of the in-phase synchronized behavior. Thus, (a) synchronization is achieved usually within a few oscillatory cycles, (b) differences of natural frequencies are compensated, (c) edge (boundary) effects are compensated, (d) an increase of the relaxation character or the coupling strength eliminates phase differences, (e) an almost synchronous response is expected for relaxation oscillators with more than two time scales, and, (f) the almost synchronous response can be order preserving or order reversing depending on the coupling strength and the time scale threshold. As far as it concerns coupled fast inhibitory relaxation oscillators the typical response can be out-of-phase or antiphase as well as more exotic [13–15].

All the above features were observed also numerically for simple models of neural oscillators. In the present paper, the synchronization modes as well as the transition features to in-phase or out-of-phase locking are studied experimentally for a system consisting of a number of coupled relaxation oscillators which can mimic excitatory or inhibitory neurons, depending on the architecture of the network. The nature of the system is electrochemical; each oscillator is an electrode pair which oscillates periodically within a region of applied potential differences. The only medium of communication between oscillators is the electrolytic solution, that is, the possible ionic movement due to diffusion and migration and associated potential variations. The experimental system is $Fe|H_2SO_4, CuSO_4|Cu$, i.e., the anodes and cathodes are iron and copper electrodes, respectively, and the electrolytic medium is an aqueous solution of sulfuric acid and copper sulfate.

The kinetic analogy between the spatiotemporal response of electrochemical and electrophysiological oscillations and nervous stimulations has been observed and studied long ago [16,17] and discussed in the past [18,19]. In the following, it will be shown that these similarities can be extended even further. The first objective of this paper is to study whether the present experimental system falls into the category of coupled relaxation oscillators described by the theoretical work of Somers and Kopell [9,10] and further elaborated by Izhikevich [12]. Indeed, we will demonstrate experimentally that assemblies of relaxation oscillators synchronize their jumps even for big differences of natural frequencies. The compensation of differences is manifested also by an independence on boundary effects, i.e., natural frequencies of edge oscillators under chain configurations. Additionally, the synchronized response is achieved within a very small time interval (within a few oscillatory cycles). The second objective of this paper is to investigate the spatiotemporal states emerging through the coupling of large assemblies of such identical oscillatory electrode pairs and to determine how

*Email address: antonis@chem.saitama-u.ac.jp

these dynamic modes are affected or controlled by the geometric configuration of the system. It will be shown experimentally that the synchronized behavior and the associated spatiotemporal response is fully determined by the geometric configuration of the assembly; the synchronization modes are defined by the architecture of the network and a simple set of rules.

It must be noted that coupled electrochemical oscillators have been studied extensively in the past. In most of these works, the main objective was to relate the coupled response of discrete oscillators to the spatially extended behavior, since collections of coupled oscillators are considered as a simplified intermediate tool between local and spatially extended systems [20]. Some systems studied under this perspective were iron arrays in sulfuric acid [21–24], rotating or nonrotating iron or cobalt disks embedded in the same insulating surface [25,26], coupled iron wires [27,28], chaotic iron oscillators [29], assemblies of nickel oscillators [30–32], and coupled hydrogen peroxide oscillatory reduction on platinum electrodes [33]. It is now evident from these studies that coupling in electrochemical systems takes place mainly due to migration currents [34–37] (even though other possibilities are still discussed in recent publications [30]). In the present paper, we will not emphasize on the electrochemical processes or the microscopic coupling mechanism.

In order to facilitate the description of the phenomena, let us introduce some terminology. A pair of electrodes where the one is acting as an anode and the other as a cathode, under a fixed potential difference V_i will be designated as cell i, where $i=1,2,\ldots,N_{\max}$ is an arbitrary integer chosen to name the cell, and $N_{\max}$ the maximum number of cells. The distance between electrodes of a cell will be d_i whereas the distance of adjacent electrodes of different cells will be $l_{i,j}$. The natural period of the cell i will be T_i^*. Electrodes lying within a distance $l_{i,j}$ are said to define a *node*. A collection of N cells will be named a *set*. In the present case, the maximum number of cells allowed by the instrumentation is $N_{\max}=30$. The number of nodes for a given set depends on the geometrical configuration. A subset of cells oscillating with the same phase and period will be called a *group*. The symbol T_i will be used for the period of group i whereas $\Delta t_{i,j}$ will be the time delay and $\Delta\phi_{i,j}$ (mod 1) the phase difference between group i and j. Obviously, the maximum number of possible groups is $N_{\max}$ in the case when all cells are locked out of phase.

II. EXPERIMENT

The iron electrodes were made from Fe wires (Nilaco Co., 99.5%) of 1 mm diameter. The copper coil electrodes were made from 40 cm length Cu wires (Nilaco Co., 99.9+%) of 1 mm diameter. Iron electrodes were completely covered by an insulating film except for a cylindrical area of $\alpha=2$ mm height at $\approx$2.5 cm from the bottom of the wire. Reaction is expected to take place only on this ring-shaped area. Iron electrodes were used as anodes and copper electrodes as cathodes in a two-electrode electrochemical arrangement. A schematic example of the experimental setup is shown in Fig. 1(a) for an arrangement consisting of two cells.

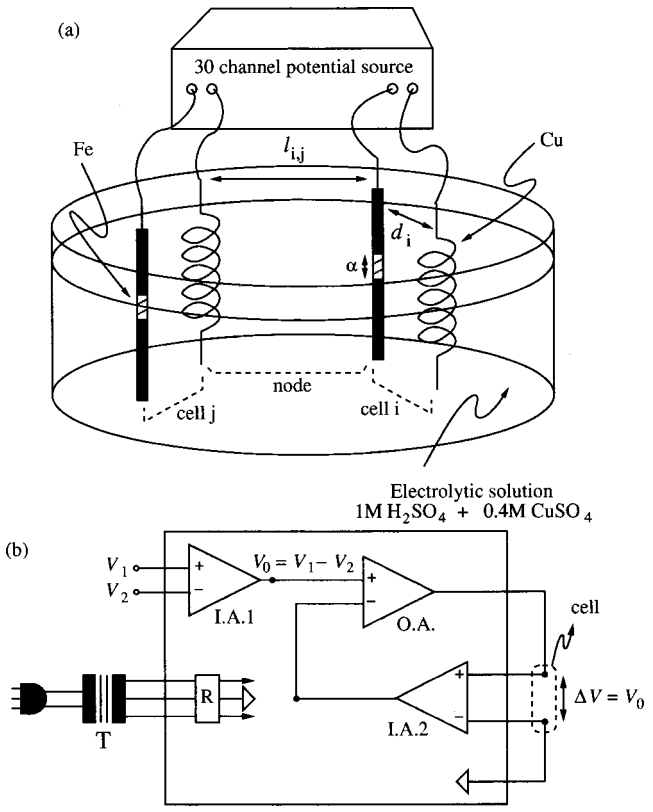

FIG. 1. (a) Schematic experimental setup for a set consisting of two cells ($N=2$): The Fe and Cu electrodes are anodes and cathodes, respectively. The reacting surface of the Fe electrodes has height α. The distance between an anode and a cathode for cell i is d_i. The distance between adjacent electrodes is $l_{i,j}$. Electrodes within a distance $l_{i,j}$ define a node. (b) Simplified schematic representation of one channel of the potential source. T: transformer, R: voltage regulator, IA: instrument amplifier, OA: operational amplifier.

The position of the electrodes (parameters d_i and $l_{i,j}$) was fixed with a specially designed acrylic plate where holes of 1 mm diameter were drilled thus forming a grid of minimum distance 0.5 cm. The potential difference for each cell was held constant by using a multi-channel potential source (Huso Electrochemical System 9052). The maximum number of channels supported by this instrument was $N_{\max}=30$. The output circuit of each channel was electromagnetically isolated from the source and other channels using transformers. The isolation resistance was >100 MΩ at ± 10 V, and the leaking current was <30 pA. The signals of current, potential, and clock were fed into an analog-to-digital converter and stored in a personal computer (NEC, PC-9821Xa200/W30R) at sampling intervals $\delta t=0.01$ s. A schematic representation of one channel of the potential source is shown in Fig. 1(b).

Experiments were carried out in a mixture of 1 M H_2SO_4 and 0.4 M $CuSO_4$ solution, diluted from concentrated sulfuric acid and dissolved copper (II) sulfate pentahydrate (Wako Pure Chemical Industries Ltd.). The diameter of the reaction bath was 30 cm and its depth 6 cm.

The process of a typical measurement was as follows: The solution was poured into the reaction bath up to 5 cm depth.

The electrodes were arranged on the acrylic grid in the desired configuration and the height of the reaction surfaces of the iron electrodes were carefully made even. The set was placed into the solution and the applied potential V_i was scanned towards the passive state up to $V_i = 1500$ mV. Then the applied potential was shifted to a desired value and a simultaneous measurement of the current flowing through each cell was performed.

In order to ensure that all oscillatory pairs were identical, before each experiment the equilibrium potential of all electrodes was measured versus a reference electrode in a solution identical with the electrolyte of the system. Only electrodes whose potential difference was $< \pm 1$ mV were used. As a second check for the identity of oscillatory pairs, the period of each uncoupled oscillator was measured for the applied potential differences under study. The duration of the spatiotemporal patterns was >30 min.

III. RESULTS

A. Synchronization, transitions, and boundary effects

A single cell consists of only an iron ring and a copper coil functioning as an anode and cathode, respectively. For reference, the distance between the anode and the cathode is $d = 5$ cm. Under fixed potential difference conditions, a single cell oscillates in a potential window extending from $V \approx 215$ to ≈ 245 mV. For $V < 215$ mV the system is on a steady state (SS_1) where the current attains a constant value, $I \approx 7.5$ mA. For $V > 245$ mV the system lies on another steady state (SS_2) where the current is almost zero. Within the oscillatory region, the current oscillates periodically. The amplitude as well as the period of the oscillations increases for increasing values of V.

A typical transition from SS_1 to a limit cycle is shown in Fig. 2(a). By increasing V, a transition to full blown oscillations is observed at $V = 218$ mV. An example of the relaxation periodic oscillations for $V = 230$ mV and $T^* = 14.29$ s is presented in Fig. 2(b). Each oscillatory cycle consists of a silent (passive) phase, an active phase, a fast transition from the silent to the active state, and a moderately fast transition from the active to the silent phase. It must be noted also that the cell always rests on the silent phase for a very long time in comparison with the active phase, for any value of V, i.e., the cell is predominantly silent. By decreasing V from within the oscillatory region, a transition to SS_1 is observed at $V = 215$ mV and thus a small hysteresis region is observed. The existence of a hysteresis region is an indication of a subcritical Hopf bifurcation at $V_{crit} = 218$ mV, even though in some cases small amplitude oscillations (<20 mA) of small period were recorded just prior to the transition to the limit cycle. The transition from the limit cycle to SS_2 takes place at $V \approx 245$ mV, after a large increase of the period and the direct characterization of the bifurcation is difficult.

The dependence of the period, T^*, of the oscillations on V, for $d = 3$ and 5 cm, is shown in Fig. 3. It can be seen that the period increases drastically by increasing V. Essentially the same trend is observed for any value of d in the range $3 \leqslant d \leqslant 10$ cm. In the following, we will restrict our paper

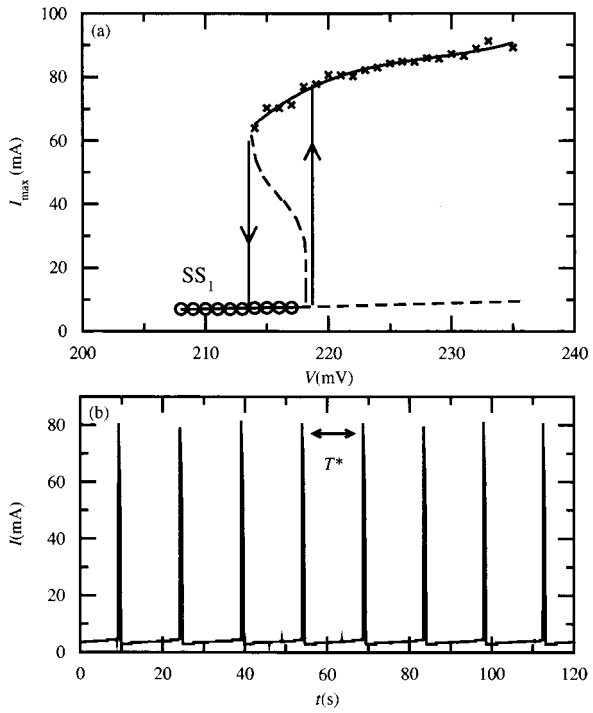

FIG. 2. (a) Bifurcation curve for a single cell. (○): stable steady state (SS_1), (×): maximum amplitude of stable oscillations, (− − −) schematic representation of unstable limit cycles. (b) Stable oscillations for $V = 230$ mV.

into the potential region over 218 mV, where the oscillations are always of relaxation type and the stable steady state SS_1 does not coexist with the limit cycle.

The most simple set consists of two cells ($N = 2$) arranged in a linear configuration. Under this arrangement only electrodes within a distance $l_{1,2}$ interact, thus, forming one node. If the node consists of two electrodes of the same kind (both anodes or both cathodes), as shown in Fig. 4(a), the two cells oscillate with the same period and phase and thus the system is synchronized. If the set is viewed as an approximation of a spatially distributed system, then it can be said that the behavior of the set is homogeneous in space. The spatial homogeneity of the set can be seen in the binary representation of Fig. 4(b), for $V_i = 227$ mV, where dark re-

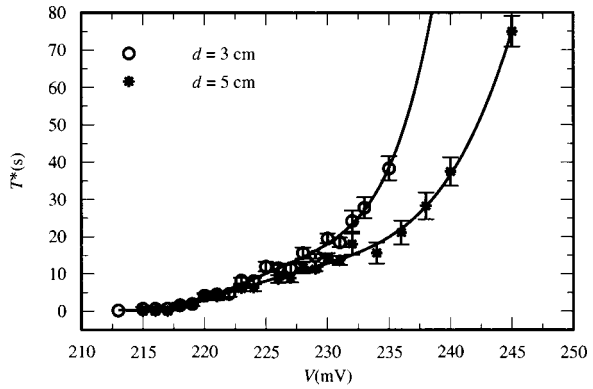

FIG. 3. Variation of the oscillations period T^* with applied potential V for two different values of d.

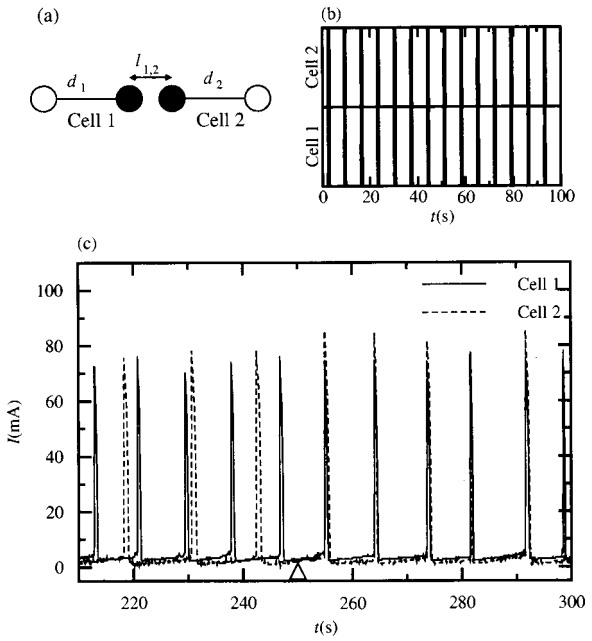

FIG. 4. (a) Two coupled pairs in linear arrangement, with two interacting anodes (black circles) and (b) coupled response for $V_i = 227$ mV. (c) Transition to synchronization for $T_1^* = 8.6$ s and $T_2^* = 12.5$ s. At the arrow, the physical obstacle is removed and coupling is effective. $l_{1,2} = 0.5$ cm, $d_i = 5$ cm.

gions correspond to an active phase (high current) and white regions correspond to silent phase (zero current). Synchronization for $N = 2$ is observed for all distances in the region $l_{1,2} < 3$ cm. For $3 \leqslant l_{1,2} < 5$ cm, more complex synchronization patterns appear and for $l_{1,2} \geqslant 5$ cm, a drifting response is observed. Once again, we will restrict our study in the region $l_{1,2} < 3$ cm where identical or almost complete synchrony is observed.

It must be pointed out that synchronization of this set seems to be independent of the initial conditions. Of course the validity of this statement is difficult to be verified experimentally but a very big number of experiments supports this observation. Thus, exactly the same features are observed when Cells 1 and 2 are shifted simultaneously from the passive to the oscillatory region, or if Cell 1 (Cell 2) is turned first to the oscillatory region and then Cell 2 (Cell 1). Also, the set is synchronized for any value of the applied potential within the oscillatory region.

The transition from uncoupled response to synchrony can be explored by inserting an acrylic plate between the two interacting electrodes. The length of the acrylic plate was 9 cm, its hight 6 cm and its width 0.2 cm. The presence of this long physical obstacle ensures complete electric and mass isolation of the two cells. As can be seen in Fig. 4(c), in the presence of the acrylic plate, cells oscillate independently with different periods, $T_1^* = 8.6$ s and $T_2^* = 12.5$ s. At $t = 250$ s the acrylic plate is removed, coupling becomes effective and cells are synchronized. It can be seen also that synchronization is achieved within the first oscillatory cycle. Also, cells compensate the differences of their period and oscillate with a common period, $T_1 = 10$ s. The compensation of the period differences is observed even when cells

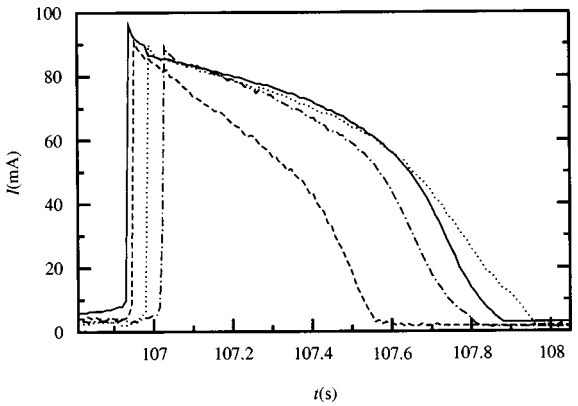

FIG. 5. Effect of coupling strength on the phase difference during synchronization, $V_i = 228$ mV. Solid line: cell 1, dashed line: cell 2, $l_{1,2} = 0.5$ cm, dotted line: cell 2, $l_{1,2} = 1$ cm, dashed-dotted lines: cell 2, $l_{1,2} = 2$ cm.

oscillate with period differences >20%.

The examples presented in Fig. 4, clearly suggest that a set of two cells becomes phase locked by synchronizing its jumps from the silent to the active phase. Nevertheless, the response is not completely (or identically) synchronized. There is a phase difference between cells, which is always a lot smaller than the order of the period or the active phase. If the distance between cells $l_{1,2}$ is considered as a measure of the coupling strength, it can be seen that the phase difference between synchronized cells decreases as the coupling strength increases. An example of this effect is shown in Fig. 5, for three sets consisting of two interacting cells. For weak coupling strength ($l_{1,2} = 2$ cm, dashed-dotted line), the phase difference between synchronized cells is rather big. The set is almost synchronized, that is, the cells cross the threshold from the silent to the active phase at time differences which are small compared to the period of the oscillations [11,38]. As the coupling becomes stronger ($l_{1,2} = 1$ cm, dotted line), the phase difference becomes smaller. Even for strong coupling ($l_{1,2} = 0.5$ cm, dashed line), cells synchronize almost completely their jumps, but there is still a small delay to this transition.

Since the coupled response is almost synchrony, it is interesting to explore whether the behavior is order preserving or order reversing. In the order preserving case, if Cell 1 is the one jumping first from the silent to the active phase and Cell 2 is the one following, this sequence is repeated throughout the time evolution of the system. In the order reversing case, if Cell 1 is the first and Cell 2 follows, then, during the next firing, Cell 2 is the first and Cell 1 follows, etc. In a set consisting of two cells, both order preserving and order reversing response is observed. Hence, for strong coupling ($l_{i,j} \leqslant 1$ cm) and low V_i values ($V_i \lesssim 225$ mV the almost synchronous response is order reversing. An example of the orientation reversing behavior is shown in Fig. 6(a) for $l_{1,2} = 0.5$ cm and $V_i = 219$ mV. It can be seen that Cell 1 fires first but dies last during the first event. During the second event, Cell 2 fires first but dies last. This sequence of events repeats itself in time. On the other hand, for weaker coupling ($l_{i,j} > 1$ cm) or high values of V_i ($V_i > 225$ mV) the

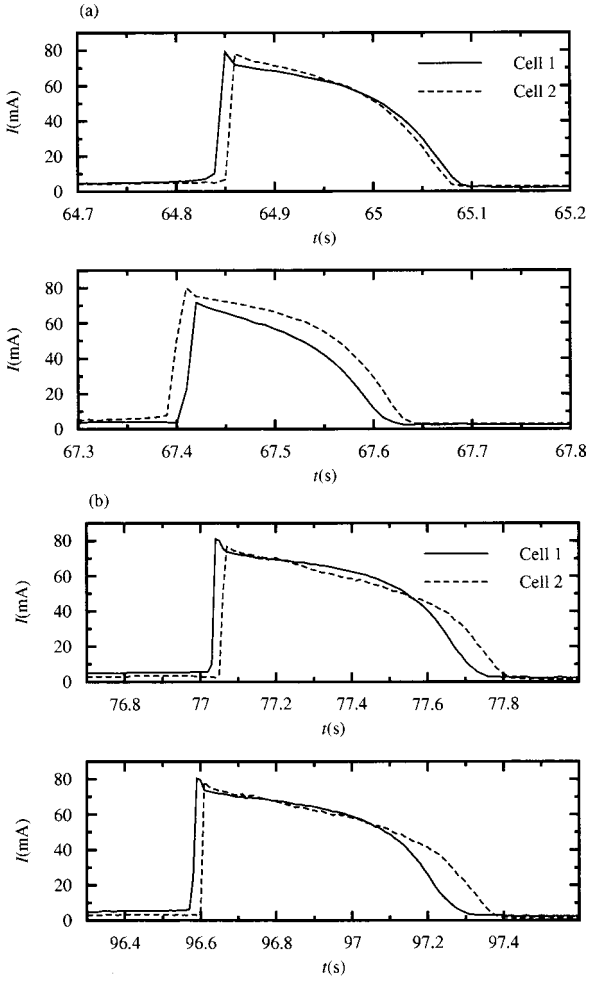

FIG. 6. (a) Two consecutive firing pairs of the order reversing response for $V_i=219$ mV, (b) two consecutive firing pairs of the order preserving response for $V_i=230$ mV. In both cases $l_{1,2}=0.5$ cm.

response is order preserving. An example of the order preserving response is shown in Fig. 6(b) for $l_{1,2}=0.5$ cm and $V_i=230$ mV. In this case, Cell 1 fires first but also dies first during the first event. During the second event the same sequence is observed, which repeats itself in time.

The experimental results concerning a set of two cells indicate that the system is synchronized rapidly albeit large differences in natural frequencies. Here we show that differences of the cells at the ends (boundaries) of a linear arrangement versus the cells at the middle are also compensated. The arrangement consist of three cells ($N=3$), as shown in Fig. 7(a). In order to ensure that interactions are mainly through neighboring electrodes we set $l_{1,2}=l_{2,3}=1.5$ cm. Under this configuration the distance between Cells 1 and 3 is 3 cm, so interactions between the two boundary electrodes must be minimal. Also, the middle cell interacts both with Cells 1 and 3, whereas the boundary cells interact mainly with Cell 2. An example of the transition to synchrony for this set is shown in Fig. 7(b). In the presence of obstacles isolating the three cells, cells oscillate independently with different periods, $T_1^*=16.6$ s, $T_2^*=13.2$ s, and $T_3^*=15.8$ s. At $t=210$ s the coupling is made effective; the

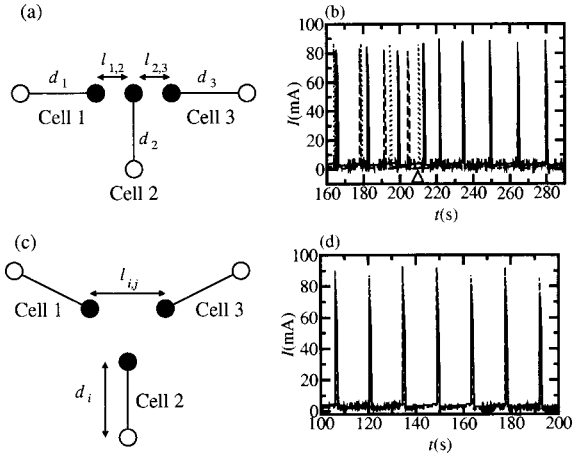

FIG. 7. (a) A chain of three cells, $l_{1,2}=l_{2,3}=1.5$ cm, $d_i=5$ cm and (b) transition to synchrony. The natural periods of the cells are $T_1^*=16.6$ s, $T_2^*=13.2$ s, and $T_3^*=15.8$ s. At the arrow, the physical obstacles are removed and coupling is effective. (c) A ring of three cells, $l_{i,j}=1.5$ cm, $d_i=5$ cm, and (d) synchronized response (traces overlapped).

chain is rapidly synchronized, and period differences are completely diminished. The synchronized set oscillates with period $T_1=14.3$ s.

The above results suggest that chains and rings consisting of the same number of cells must synchronize in a similar manner, since boundary effects are not important. In order to verify this hypothesis, a ring consisting of three cells is investigated, under the configuration presented in Fig. 7(c). Under this arrangement (no boundaries) the system is synchronized in exactly the same manner with a chain, as can be seen in Fig. 7(d). The natural periods of the cells are chosen to be almost the same as in the example of Fig. 7(b), $T_1^*=15.5$ s, $T_2^*=14$ s, and $T_3^*=15$ s. Cells are rapidly synchronized and the period differences are compensated. The synchronized set oscillates with period $T_1=14.4$ s, almost the same with the synchronized set under the chain configuration.

Synchronization of rings is also observed for $N>3$, e.g., in the case of a regular hexagon configuration. Under this geometry six cells are used ($N=6$). The distance between electrodes belonging to the same cell is set to $d_i=5$ cm, that is, $d_1=d_2=\cdots=d_6$. The distance between adjacent electrodes is set to $l_{i,j}=1$ cm, as can be seen in Fig. 8(a). Under this configuration only electrodes lying within a distance $l_{i,j}$

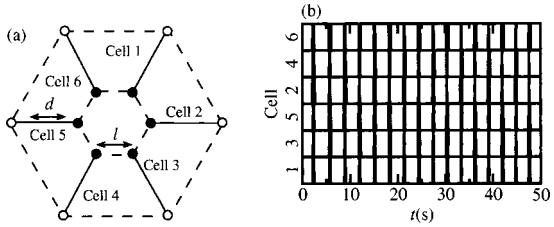

FIG. 8. (a) Regular hexagon set with one node. The node consists of anodes only. (b) Binary representation of the spatiotemporal response, $d_i=5$ cm, $l_{i,j}=1$ cm, and $V_i=225$ mV.

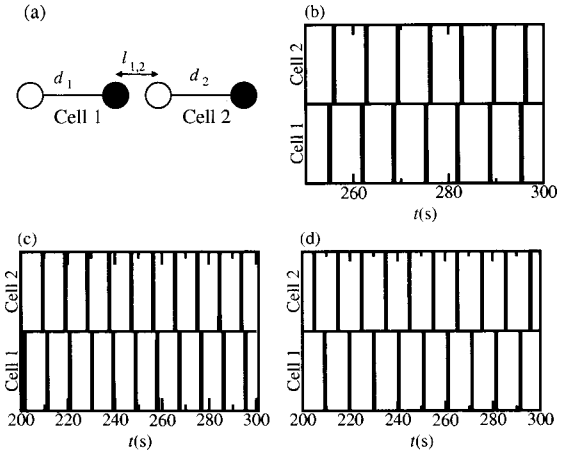

FIG. 9. (a) Two coupled pairs in linear arrangement, with interacting anode (black circle) and cathode (white circle), (b) out-of-phase synchronization for $V_i=224$ mV. Bistability between, (c) out-of-phase synchronization, and (d) antiphase synchronization for $V_i=230$ mV. $l_{1,2}=0.5$ cm, $d_i=5$ cm.

are expected to interact since the rest of the electrodes are considerably far away from each other. Thus, the number of nodes in this regular polygon arrangement is one. The potential of each cell is set to a value V_i within the oscillatory region, and $V_1=V_2=\cdots=V_6$. This configuration can be considered as all-to-all coupling of the six cells.

When the node consists of electrodes of a single kind [all anodes or all cathodes, Fig. 8(a)] all cells oscillate periodically in phase. An example of this synchronized behavior is shown in Fig. 8(b) for $V_i=225$ mV. It is obvious from this figure that in spite of initial differences, all cells oscillate homogeneously with the same period and phase thus forming one group where $T_1=2.92$ s.

B. Synchronization modes induced by geometry

In the previous section it was shown that when relaxation oscillatory cells are coupled through electrodes of the same nature, i.e., the nodes consist of only anodes or cathodes, the response is almost synchronized. Cells tend to synchronize their jumps from the silent to the active phase and the time difference of the jumps is always smaller than the period. In this section, it will be shown that the coupled response changes drastically if nodes consist of electrodes of different nature. In this case, interactions impede the generation of oscillations and stable in-phase synchronous response is not observed.

A typical configuration of a set consisting of two cells is shown in Fig. 9(a). The only node of this set consists of an anode and a cathode. Under this configuration two different kinds of synchronized response are observed which are both out of phase. During the first kind of synchronization, cell i and cell j are out of phase but cell j jumps to the active phase as soon as cell i turns to the silent phase. The second kind of synchronization is antiphase; cells oscillate with the same period but with a phase difference $\Delta\phi_{i,j}\approx 0.5$. An additional feature is that while cell i is on the active and cell j on the silent phase, a small decrease of the current of the silent phase is observed which persists while the other cell is active. This decrease of the current is of the order of 1 mA.

Representative examples of the out-of-phase response for $l_{1,2}=0.5$ cm and $d_i=5$ cm are shown in Figs. 9(b) and 9(c). As can be seen, for $V_i=225$ mV, cells oscillate out of phase and cell j jumps to the active phase soon after cell i reaches the silent phase. Cells develop a constant phase difference, $\Delta\phi_{1,2}=0.14$, and become synchronized. A similar pattern is followed in Fig. 9(b) for $V_i=230$ mV, where now the constant phase difference is $\Delta\phi_{1,2}=0.18$. An example of the antiphase synchronization is shown in Fig. 9(d) for $V_i=230$ mV where the phase difference is $\Delta\phi_{1,2}=0.48$. In all cases presented in Fig. 9, it can be stated that the behavior is inhomogeneous in space, if the set is viewed as an approximation of a spatially distributed system.

Generally, antiphase response is observed for high values of V_i (i.e., long periods, T^*) while out-of-phase behavior is observed for low values of V_i. This observation, supported by a big number of experiments, has also exceptions, as can be noticed by comparing Figs. 9(c) and 9(d). Thus, even though V_i is the same in both experiments, either out-of-phase or antiphase synchronization can be observed, possibly depending on the initial conditions. Nevertheless, for high V_i the response presented in Fig. 9(c) is very rare.

Out-of-phase synchronization can lead to grouping (or clustering) when the set consists of more than two cells. A simple symmetric set arrangement for $N>2$, is the regular hexagon configuration. Once again, six cells are used ($N=6$) and the distance between electrodes belonging to the same cell is set to $d_i=5$ cm. The distance between adjacent electrodes is set to $l_{i,j}=1$ cm, as shown in Fig. 10(a). Similar to the case $N=6$ presented in the previous section, the six cells are all-to-all coupled.

Initially, all cells are expected to oscillate with slightly different periods and different phases due to different initial local electrolytic conditions and experimental imperfections. During the course of oscillations, cells interact through the electrolytic solution within the node. Once again, the resulting response of the set is determined by the electrochemical origin of the neighboring electrodes, similar to the case $N=2$ presented in Fig. 9. Hence, the set is divided into two groups; within each group, cells oscillate with the same period and almost the same phase, but different groups oscillate out of phase. Typical examples of this behavior are shown in Figs. 10(b)–10(d). For $V_i=224$ mV [Fig. 10(b)] the period of each group is $T_1=T_2=3.02$ s. In this example the phase difference, $\Delta\phi_{1,2}\approx 0.24$, is constant corresponding to a delay $\Delta t_{1,2}=0.72$ s. Clearly, Cells 1, 3, and 5 constitute one group whereas Cells 2, 4, and 6 belong to another group. Similar trend is observed for $V_i=228$ mV [Fig. 10(c)] where $T_1=T_2=9.47$ s and $\Delta t_{1,2}=1.18$ s ($\Delta\phi_{1,2}\approx 0.12$). The set is divided into two groups for even higher values of V_i. As can be seen in Fig. 10(d), Cells 1, 3, and 5 continue to form one group whereas Cells 2, 4, and 6 form a second group but the system tends to antiphase synchronization in a slower rate.

The effect of V_i on the rate of convergence to synchrony can be seen in Fig. 10(e), where the time delay, $\Delta t_{1,2}$ corresponds to the peak-to-peak time interval between Group 1

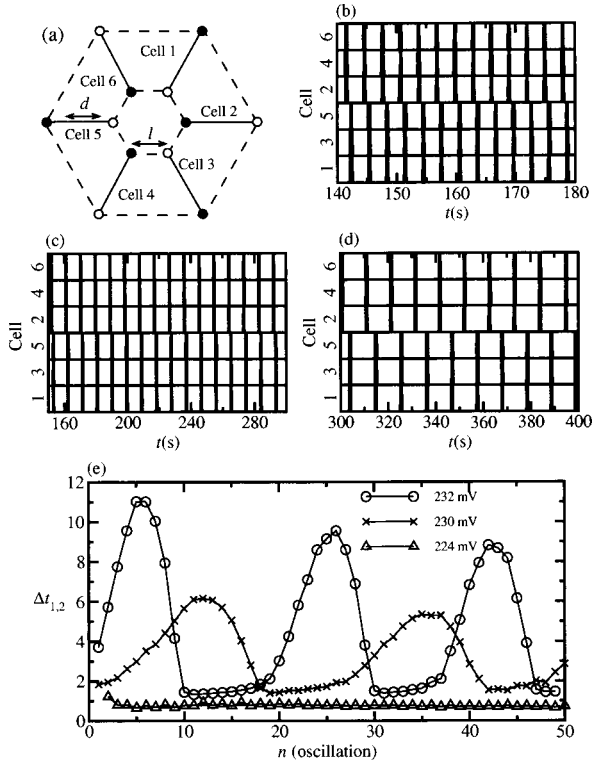

FIG. 10. (a) Regular hexagon set with one node. The node consists of alternating anodes (black circles) and cathodes (white circles). Binary representation of the spatiotemporal response for (b) $V_i=224$ mV, (c) $V_i=228$ mV, (d) $V_i=230$ mV. (e) Time delay between Group 1 and 2 for various V_i. $d_i=5$ cm, $l_{i,j}=1$ cm.

and 2, and n corresponds to the nth peak of the time series. For low values of V_i, groups oscillate with small phase difference and are rapidly synchronized. As V_i increases, the rate of convergence is slow, the phase difference varies slowly in time but it is always bounded, i.e., groups never overlap. Using some definitions [39,40] it can be stated that for the examples presented in Fig. 10, cells belonging to the same group are synchronized almost identically, since their phase-space variables are almost identical. Also, groups are lag synchronized.

The examples presented in Fig. 10 reveal that the synchronization modes and the resulting spatiotemporal patterns are determined by the architecture of the network. This hypothesis can be tested for rather complex, yet symmetric, geometrical configurations, like a set in a ''star'' arrangement, consisting of 24 cells ($N=24$). As can be seen in Fig. 11(a), the number of nodes in this set is 13, since $d_i=5$ cm and $l_{i,j}=0.5$ cm. The central node consists of six electrodes, whereas the perimeter and outer nodes consist of five and two electrodes, respectively. Individual nodes lie far away from each other, hence, we expect that cells interact only through electrodes belonging to the same node.

The response of the ''star'' set is very unique when electrodes belonging to the same node are alternating anodes and cathodes, Fig. 11(a). In this case, for high values of V_i, the set is divided into three distinct groups. Group 2 and Group 3 consist of nine cells, whereas Group 1 consists of six cells, as can be seen schematically in Figs. 11(b), 11(c), and 11(d).

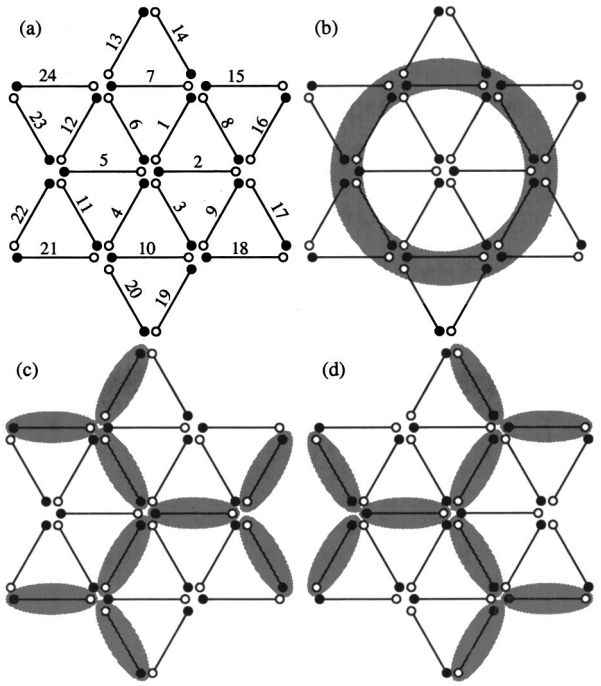

FIG. 11. (a) Star set with 13 nodes ($N=24$), (b) Group 1, (c) Group 2, and (d) Group 3.

Within each group cells oscillate with the same period and phase but groups oscillate out of phase. Thus, if Group 1 (Cells 7–12) fires first its oscillatory pulse, Fig. 11(b), then Group 2 (Cells 2, 4, 6, 13, 16, 17, 20, 21, and 24) will fire, Fig. 11(c), and after that, Group 3 (Cells 1, 3, 5, 14, 15, 18, 19, 22, and 23) will fire an oscillatory pulse, Fig. 11(d). Then, Group 1 will oscillate again and this series of events will repeat itself in time.

Typical examples of the response of the ''star'' configuration are presented in Fig. 12. For low values of V_i, the spatiotemporal response is complex and groups are not formed, as can be seen in Fig. 11(a) for $V_i=227$ mV. By increasing the applied potential difference, the set is divided into groups according to the schematic of Fig. 11. Thus, for $V_i=229$, 230, and 232 mV three distinct groups are formed, as can be seen in Figs. 12(b)–12(d).

IV. DISCUSSION

Assemblies of almost identical oscillatory electrode pairs are synchronized when they are coupled through the electrolytic solution. Due to experimental limitations, natural frequencies and initial phases are always different, but coupling leads to collective synchronization, similar to biological oscillators which can spontaneously synchronize to a common frequency even if there is a distribution of natural frequencies among the population [2].

Here, we will attempt a comparison of the experimental results presented in the proceeding sections with the theoretical work concerning coupled relaxation oscillators of neurolobiological interest [9,10,12,14,15]. The main characteristic of coupled excitatory relaxation neural oscillators was proved to be their rapid transition to synchrony. This result

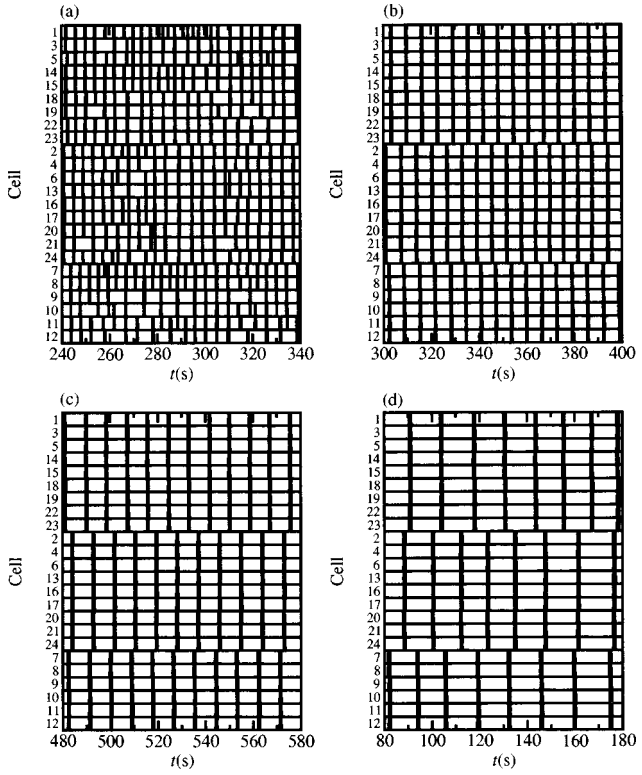

FIG. 12. Binary representation of the spatiotemporal response for the star configuration, $d_i = 5$ cm, $l_{i,j} = 0.5$ cm. (a) $V_i = 227$ mV, (b) $V_i = 229$ mV, (c) $V_i = 230$ mV, (d) $V_i = 232$ mV.

was also shown to be valid in numerical calculations of simple neural oscillator models [9,10]. The present experimental system presents exactly the same characteristics. As was shown in Figs. 4(b) and 7(b), couples or arrays of oscillatory cells synchronize almost identically within only few oscillatory cycles. Another important characteristic of coupled relaxation neurons is that they compensate their period differences. This compensation proved to be valid numerically even for period differences up to 50% [10]. In the present paper, it was shown experimentally in Figs. 4, 7, and 8 that this is also true for coupled relaxation electrode pairs; cells tend to forget all initial differences and synchronize into a common frequency. This trend was observed experimentally for differences exceeding 20%. Differences of edge neurons (boundaries) in chain configurations were also proved to be eliminated during coupling. The same trend was observed in the present system (Fig. 7) where the response of a chain and a ring set consisting of three cells were shown to be apparently the same.

Identical synchronization, i.e., exact simultaneous jump from the silent to the active phase, is expected to occur either for cells lying on their relaxation limit, satisfying the ''compression hypothesis'' and under Heaviside-type excitatory coupling [9,10] or for any kind of excitatory coupling, provided that relaxation oscillators are very weakly coupled [12]. Moving away from the relaxation limit or making the coupling more ramplike, a phase difference is developed between relaxation neurons, leading to wave propagating response. Additionally, rigorous conditions were proved to exist, under which the almost synchronous response is the only stable solution for a pair of coupled relaxation oscillations evolving in more than two time scales [11]. In the present paper, it was also experimentally shown that relaxation cells are actually almost synchronized. The jump time delay was always smaller than the oscillations' period and tended to smaller values as the coupling strength increased (Fig. 5). In theory, the almost synchronous solution can be order preserving or order reversing depending on the relative magnitude of the time scale threshold and the coupling strength. Of course, in the present experimental system there is not any direct way to control the time scale threshold but it was systematically observed that for strong coupling and low values of V_i the almost synchronous response is order reversing, Fig. 6(a). On the other hand, high V_i values and/or weaker coupling leads to order preserving synchronization, Fig. 6(b).

Coupling of identical periodic oscillators does not always lead to identical synchronization. Even simple diffusive coupling of identical periodic oscillators can dephase the individual oscillators and cause out-of-phase or even complex oscillatory behavior. This kind of exact response was initially predicted [20] and later confirmed by numerical experiments of coupled neural oscillators [41]. Recently, identical results were obtained for a caricature model of coupled electrochemical oscillators [42]. The main cause of dephasing in those cases is a strong deformation of the phase flow in the vicinity of the limit cycle which can lead to bursting oscillations as far as a homoclinic limit cycle exists. In the present paper, we show a different mechanism leading to dephasing. Cells oscillate out of phase if only the geometric configuration of the system is changed. Thus, if the interacting electrodes are of a different kind the response will be dephased whereas if the interacting electrodes are of the same kind the system will be synchronized in phase. The response of the system for interacting electrodes of a different kind resembles the behavior of coupled inhibitory neurons [13–15].

This simple rule determines also the grouping (or clustering) of the cells. Thus, the number of groups as well as the cells participating in each group is fully determined by the nature of the electrodes in each node; neighboring cells interacting through electrodes of the same kind will belong to the same group and groups will oscillate out of phase. This allows us to predict the qualitative features of the spatiotemporal patterns or produce specific spatiotemporal patterns at will.

Among the large amount of work concerning relaxation neurons, there are many examples where excitatory coupling leads to antiphase response [43] or fractured synchrony [10,12]. On the other hand, there are several cases where inhibition synchronizes neural firing [7,15,44]. In the present paper, though, antiphase response is never observed when cells are coupled through electrodes of the same nature (imitating excitatory connections). Also, in-phase synchronization is never observed when cells are coupled through electrodes of different nature (imitating inhibitory connections). Nevertheless, the existence and stability of these states cannot be excluded. A systematic investigation of the effect of the initial conditions, electrolyte composition, and external perturbations is in progress in our laboratory, in order to

reveal additional synchronization modes.

As a conclusion, it can be stated that coupled electrode pairs of relaxation character closely resemble the response of coupled relaxation neural oscillators. This was verified by a series of comparisons between the present experimental system and the theoretical predictions which revealed that coupled relaxation cells of electrochemical origin can mimic many of the features of coupled relaxation neurons. Also, it was shown that networks consisting of assemblies of coupled relaxation cells can produce synchronization patterns at will by following simple configuration rules.

ACKNOWLEDGMENTS

This work was supported by the Research for the Future (RFTF) program of the Japan Society for the Promotion of Science.

[1] F. Hoppensteadt and E. Izhikevich, *Weakly Connected Neural Networks*, Applied Mathematical Sciences, Vol. 126 (Springer-Verlag, New York, 1997).
[2] P. Matthews and S. Strogatz, Phys. Rev. Lett. **65**, 1701 (1990).
[3] L. Abbott and C. Vreeswijk, Phys. Rev. E **48**, 1483 (1993).
[4] C. Vreeswijk, Phys. Rev. E **54**, 5522 (1996).
[5] D. Terman and D. Wang, Physica D **81**, 148 (1995).
[6] N. Kopell and G. Ermentrout, Commun. Pure Appl. Math. **39**, 623 (1986).
[7] C. Vreeswijk, L. Abbott, and G. Ermentrout, J. Comput. Neurosci. **1**, 313 (1994).
[8] D. Storti and R. Rand, SIAM (Soc. Ind. Appl. Math.) J. Appl. Math. **46**, 56 (1986).
[9] D. Somers and N. Kopell, Biol. Cybern. **68**, 393 (1993).
[10] D. Somers and N. Kopell, Physica D **89**, 169 (1995).
[11] A. Bose, N. Kopell, and D. Terman, Physica D **140**, 69 (2000).
[12] E. M. Izhikevich, SIAM (Soc. Ind. Appl. Math.) J. Appl. Math. **60**, 1789 (2000).
[13] P. Rowat and A. Selverston, J. Comput. Neurosci. **4**, 103 (1997).
[14] D. Terman and E. Lee, SIAM (Soc. Ind. Appl. Math.) J. Appl. Math. **57**, 252 (1997).
[15] D. Terman, N. Kopell, and A. Bose, Physica D **117**, 241 (1998).
[16] R. Lillie, J. Gen. Physiol. **3**, 107 (1920).
[17] R. Lillie, J. Gen. Physiol. **7**, 473 (1925).
[18] U. Franck, Prog. Biophys. Biophys. Chem. **6**, 171 (1956).
[19] U. Franck, Angew. Chem. **17**, 1 (1978).
[20] Y. Kuramoto, *Chemical Oscillators, Waves, and Turbulence* (Springer-Verlag, Berlin, 1984).
[21] Z. Fei, R. Kelly, and J. Hudson, J. Phys. Chem. **100**, 18 986 (1996).
[22] Z. Fei and J. Hudson, J. Phys. Chem. B **101**, 10 356 (1997).
[23] Z. Fei, B. Green, and J. Hudson, J. Phys. Chem. B **103**, 2178 (1999).
[24] I. Kiss, W. Wang, and J. Hudson, J. Phys. Chem. B **103**, 11 433 (1999).
[25] J. Bell, N. Jaeger, and J. Hudson, J. Phys. Chem. **96**, 8671 (1992).
[26] B. Rush and J. Newman, J. Electrochem. Soc. **142**, 3770 (1995).
[27] S. Nakabayashi, K. Zama, and K. Uosaki, J. Electrochem. Soc. **143**, 2258 (1996).
[28] A. Karantonis, Y. Shiomi, and S. Nakabayashi, J. Electroanal. Chem. **493**, 57 (2000).
[29] Y. Wang and J. Hudson, J. Phys. Chem. **96**, 8667 (1992).
[30] I. Kiss, W. Wang, and J. Hudson, Phys. Chem. Chem. Phys. **2**, 3847 (2000).
[31] W. Wang, I. Kiss, and J. Hudson, Chaos **10**, 248 (2000).
[32] W. Wang, B. Green, and J. Hudson, J. Phys. Chem. B **105**, 7366 (2001).
[33] Y. Mukouyama, H. Hommura, T. Matsuda, S. Yae, and T. Nakato, Chem. Lett. 463 (1996).
[34] K. Krischer, in *Modern Aspects of Electrochemistry*, edited by B. Conway, J. Bockris, and R. White (Plenum Press, New York, 1999), Vol. 32, pp. 1–142.
[35] P. Grauel, J. Christoph, G. Flätgen, and K. Krischer, J. Phys. Chem. B **102**, 10 264 (1988).
[36] J. Christoph, R. Otterstedt, M. Eiswirth, N. Jaeger, and J. Hudson, J. Phys. Chem. **110**, 8614 (1999).
[37] R. Otterstedt, N. Jaeger, P. Plath, and J. Hudson, Chem. Eng. Sci. **54**, 1221 (1999).
[38] P. Pinsky, SIAM (Soc. Ind. Appl. Math.) J. Appl. Math. **55**, 220 (1995).
[39] R. Brown and L. Kocarev, Chaos **10**, 344 (2000).
[40] S. Boccaletti, L. Pecora, and A. Pelaez, Phys. Rev. E **63**, 066219 (2001).
[41] S. Han, C. Kurrer, and Y. Kuramoto, Phys. Rev. Lett. **75**, 3190 (1995).
[42] A. Karantonis and S. Nakabayashi, Chem. Phys. Lett. **347**, 133 (2001).
[43] N. Kopell and D. Somers, J. Math. Biol. **33**, 261 (1995).
[44] X. Wang and J. Rinzel, Neural Comput. **4**, 84 (1992).